Dual reservoir structure at Soufrière Hills Volcano inferred from continuous GPS observations and heterogeneous elastic modeling

Roozbeh Foroozan,[1] Derek Elsworth,[1] Barry Voight,[2] and Glen S. Mattioli[3]

Received 14 January 2010; revised 2 February 2010; accepted 17 February 2010; published 1 April 2010.

[1] Most inversions of geodetic data for volcanic systems assume homogeneous media. Here we examine the effect of inhomogeneous media using axisymmetric finite element models of Soufrière Hills Volcano (SHV), to show that homogeneous elastic crustal models underestimate both the depth and excess pressure of the deformation source. Continuous GPS data from 1999 to 2009 are then used to infer that the SHV system has multiple crustal pressure sources. For a dual reservoir volcanic model, a deep reservoir located within the mid crust undergoes volume changes approximately an order of magnitude larger than those of the shallow reservoir. **Citation:** Foroozan, R., D. Elsworth, B. Voight, and G. S. Mattioli (2010), Dual reservoir structure at Soufrière Hills Volcano inferred from continuous GPS observations and heterogeneous elastic modeling, *Geophys. Res. Lett.*, *37*, L00E12, doi:10.1029/2010GL042511.

1. Introduction

[2] The Soufrière Hills Volcano (SHV) system has been active since 1995 and has erupted ~1 km^3 of mainly andesite material through 2009. Three distinctive effusive epochs are recognized, each comprising an active eruptive episode lasting a few years (1995 to 1998, 1999 to 2003, and 2005 to 2007) followed by relatively quiescent pauses lasting over a year [*Mattioli and Herd*, 2003; *Wadge et al.*, 2010]. The effusive epochs are characterized by ground deflations and lava dome growth while "pauses" are accompanied by ground inflations which indicate recharge of the subsurface reservoirs [*Elsworth et al.*, 2008]. As many as 10 continuous GPS (cGPS) stations have been active for the past 14 years, providing valuable information on the deformation history of SHV which can be used to investigate the magma plumbing system of the volcano [*Mattioli et al.*, 2010, B. Voight et al., The SEA-CALIPSO volcano imaging experiment on Montserrat: Aims, plans, campaigns at sea and on land, and lessons learned, submitted to *Geophysical Research Letters*, 2010].

[3] Seismic velocities obtained from the SEA-CALIPSO experiment (E. Shalev et al., Three-dimensional seismic velocity tomography of Montserrat from the SEA-CALIPSO offshore/onshore experiment, submitted to *Geophysical Research Letters*, 2010; Voight et al., submitted manuscript, 2010) have refined our understanding of the subsurface geological structure of SHV and has enabled us to develop models of inhomogeneous elastic media. Here, we use this new information to test the effects of inhomogeneity on inversions of geodetic data.

[4] In the following sections, we demonstrate that buried pressure sources beneath SHV within a heterogeneous elastic half space must be deeper than the depth inferred from homogenous elastic models. By introducing the "apparent depth" of the pressure source we define a correction factor to aid interpretation of results inferred from homogeneous models of SHV. This concept is then applied to demonstrate the existence of multiple pressure sources at different depths under the SHV volcanic system as constrained by continuous Global Positioning System (cGPS) data. The geometry and volume changes of this system are explored using the new method of GPS data analysis presented here.

2. Homogenous Versus Inhomogeneous Media Models

[5] We explore the role of inhomogeneities in modulating the misfit between geodetic observations and modeled response [*Bianchi et al.*, 1987; *Trasatti et al.*, 2005; *Crescentini and Amoruso*, 2007; *Amoruso et al.*, 2007; *Amoruso et al.*, 2008]. We use travel times of signals generated by controlled marine air-gun sources which were used in the onshore-offshore SEA-CALIPSO experiment to produce a three-dimensional (3D) model of the upper crust beneath Montserrat (Shalev et al., submitted manuscript, 2010). We develop two models to account for the crustal inhomogeneities of SHV. First, an island-wide-averaged one-dimensional (1D) model was constructed as a starting point for the 3D tomography. The Nafe-Drake formula for density variation as a function of P-wave velocity [*Nafe and Drake*, 1957; *Brocher*, 2005] is used to define the variations of the elastic modulus with depth. This calculation assumes a constant Poisson ratio (0.25) as representative of the long-term drained behavior of the rock mass. We use this 1D island-wide model to estimate the average structure of the uppermost crust. To simplify the treatment of the elastic modulus profile in Finite Element Models (FEM), an exponential association function is fitted to the modulus profile (equation (1), Figure 1a). The fit is excellent with a regression coefficient (R^2) close to unity (0.99) and results in the following distribution of modulus (E) with depth (D)

$$E(GPa) = 11.11[1.19 - \exp(-0.105D)] \quad (1)$$

[1]Department of Energy and Environmental Engineering, G3 Center and EMS Energy Institute, Pennsylvania State University, University Park, Pennsylvania, USA.
[2]Department of Geosciences, Pennsylvania State University, University Park, Pennsylvania, USA.
[3]Department of Geosciences, University of Arkansas, Fayetteville, Arkansas, USA.

0094-8276/10/2010GL042511

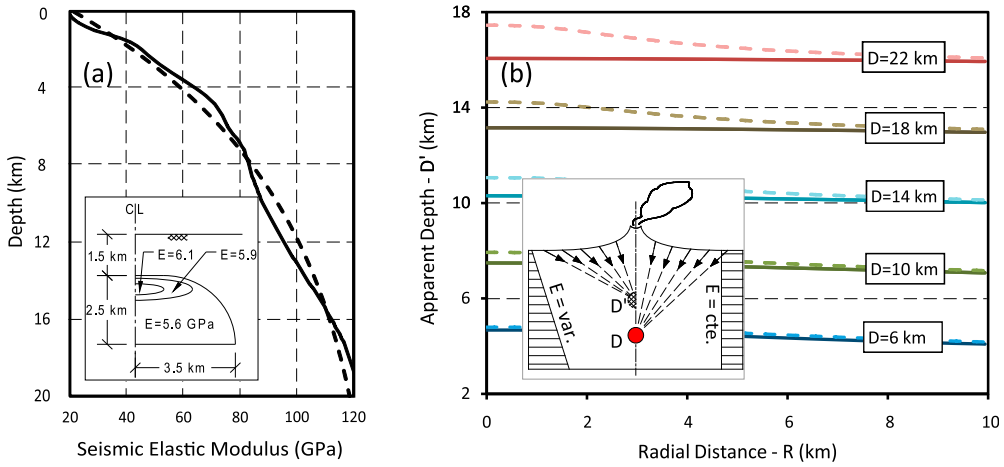

Figure 1. (a) Elastic profile from P-wave seismic profile (solid) and the exponential association function fitted to elastic modulus (dashed). Stiff core model modification shown in inset with contours of modulii centered on conduit axis. (b) The apparent depth (D′) for 1D (solid) and stiff core (dashed) models identify where the displacement vectors converge for depth-varying (inset, left) distribution of elastic modulus contrary to depth-constant (inset, right) case.

where D is the depth below sea-level in kilometers. The "effective elastic modulus" of the fractured rock mass used in the FEM models is assumed to be 0.1 of its small strain modulus [*Newman et al.*, 2001; *Bonaccorso et al.*, 2005] evaluated from seismic velocity profiles (Figure 1a). This corrects the modulus recovered from the small strain measurement of acoustic impedance to one applicable for the larger strains that accompany reservoir inflation and deflation.

[6] In our second set of models, the modulus profile used in the first set is modified to consider a region of relative higher stiffness observed underneath the crater (Shalev et al., submitted manuscript, 2010). This "stiff core" model (Figure 1, schematic inset diagram) simplifies the 3-D tomography, recovered from the SEA-CALIPSO imaging experiment, with an axisymmetric model having a region of higher stiffness, 1.5 to 4 km deep, which merges into the 1D profile deeper than 4 km.

[7] For a spherical point source in a homogeneous half space [*Mogi*, 1958], the radial (u) and vertical (w) deformation components have the relation, $u/w = R/D$, where R and D are the radial and vertical distances from a surface station to the pressure source. In other words, the surface displacement vectors for a homogeneous half space always project from the pressure source. Based on this relation, here we define the "apparent depth" of the pressure source as the depth at which the surface displacement vectors converge (Figure 1b). For the case of a point source in a homogeneous half space, the apparent source depth and the modeled source depth are identical.

[8] To examine the displacement vectors and their corresponding apparent depth for the case of an inhomogeneous half-space representative of SHV, the nonlinear elastic modulus profile (equation (1) and Figure 1a) was used in axisymmetric FEM models. Eleven models were analyzed, each comprising 1-km-diameter spherical pressure sources (magma reservoirs) at depths ranging from 4 km to 24 km incremented in 2 km intervals. The models consist of a 150 km wide (radius) by 100 km deep domain, constrained on the boundaries in their perpendicular direction and with a traction-free horizontal surface. The apparent depth (D') of the pressure source is calculated for the displacement vectors of surface points from $D' = (u/w)R$, with R up to 10 km (Figure 1b).

[9] In the 1D variable-elastic-modulus models, the apparent depth for the far-field observation points will be slightly shallower than those in the near field (Figure 1b). This is more evident for shallow pressure sources as in the case of the shallowest magma reservoir examined (D = 4 km), where the apparent depth varies from 3.3 km at the conduit to 2.6 km at 10 km radial distance. For radial distances between 2 km and 10 km, where the cGPS stations are installed, the following relationship between the apparent and modeled source depths can be formulated:

$$0.733D > D' > 0.720D \tag{2}$$

where the lower and upper bounds are radial distances of 10 km and 2 km, respectively. Since the majority of the cGPS stations are located between 3 km and 8 km from the volcano conduit the following linear relation can be considered between the apparent and modeled source depths:

$$D' = 0.73D \tag{3}$$

With this linear transformation, the inversion results from homogeneous elastic models [see, e.g., *Mattioli et al.*, 2010] may be used to evaluate depths of the pressure sources, given our simple approximation of the heterogeneous modulus profile at SHV.

[10] The same method is then further applied to the stiff core models for SHV. The apparent depths resulting from these models are also plotted in Figure 2b, as dashed lines. The stiff core results in larger u/w values and consequently a deeper apparent depth than the simple 1D heterogeneous model, especially in the near field for the case of deep pressure sources. The apparent depth in these models is a stronger function of the radial distance (R) and cannot be expressed by a simple relation as equation (2) because of the spatial heterogeneity. However, the similarity in the results between models both with and without the stiff core high-

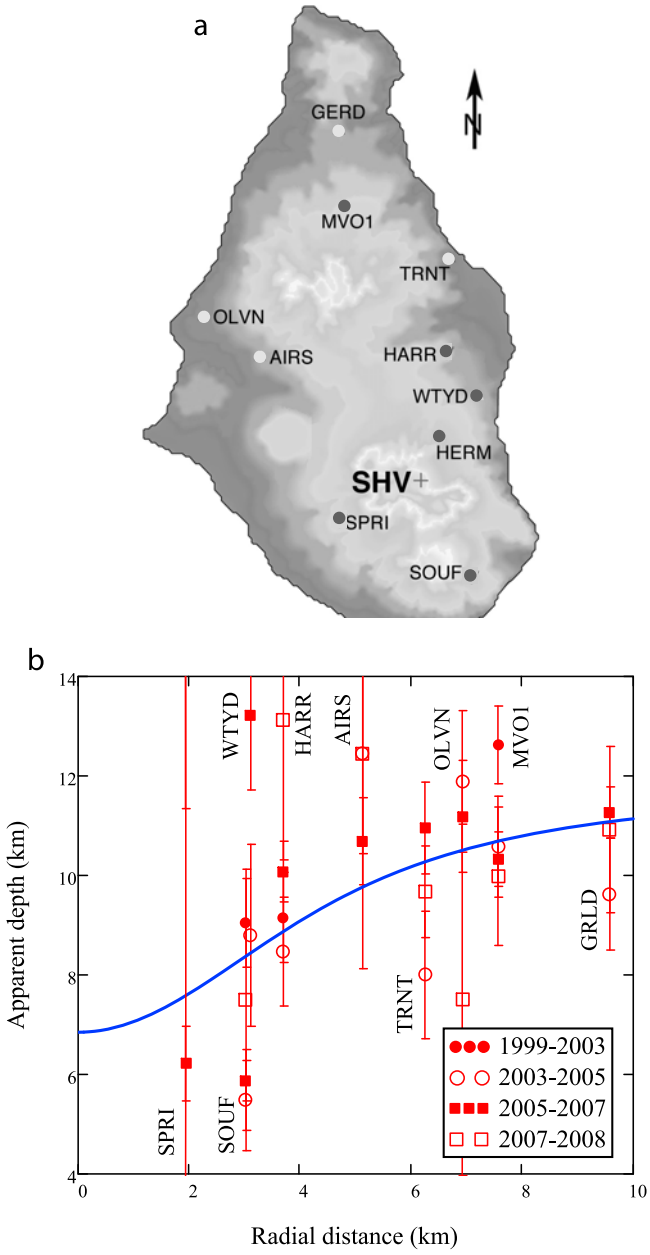

Figure 2. (a) Map of Montserrat, showing the location of the eruptive vent (SHV) and CALIPSO (light) and MVO, pre2003, (dark) stations (b) Apparent depths and 1 sigma standard deviations from the GPS velocity components (red); and the fitted model resulting from two Mogi pressure sources at 5 km and 17 km deep with 0.012 and 0.25 km^3 volume changes, respectively.

lights the inherent insensitivity of geodetic techniques to resolving structures at depth.

3. GPS Data

[11] Although GPS data have been available for SHV since 1995 [*Mattioli and Herd*, 2003; *Mattioli et al.*, 1998], the number and importantly the quality of those data has improved significantly with time. Here, we use the post-Dec-1999 data, when the volcano's second eruptive episode started. The data corresponding to the first eruptive episode (1995–1998) and subsequent pause (1998–1999) are not used due to their higher noise levels. Six cGPS stations recorded the deformation history of the island until 2003, when four CALIPSO stations were added to the network [*Mattioli et al.*, 2004]. Two eruptive episodes (1999 to 2003, and 2005 to 2007), followed by pauses have been identified since Dec 1999. The eruptive episodes are distinguished from pauses by abrupt changes in vertical velocities recorded by cGPS stations [*Elsworth et al.*, 2008]. In each of the four individual periods we analyzed (eruption-pause-eruption-pause) the average surface velocity of each recording station within the prescribed cycle together with the standard deviation are available. These measurements are reported in this volume together with a detailed description of data gathering and processing procedure [*Mattioli et al.*, 2010]. In the case of a point source, the horizontal velocity vectors should all point to the surface projection of the buried pressure source, which is likely to be proximal to the conduit. For the stations closest to the volcanic conduit (HERM, r = 1.6 km, SPRI, r = 1.9 km and WTYD, r = 3.1 km), the horizontal velocity vectors exhibit the greatest variability during some stages of eruption and pause. These deviations remain unconstrained in this work but may be due to the presence of shallow pressure sources [*Widiwijayanti et al.*, 2005] or shallow structural controls on deformation. The deviation is especially large for the closest station (HERM) where the angle between the horizontal velocity and the radial position vector of the station with respect to the volcano conduit is never smaller than 30· supporting the presence of fault-bounded structural controls on deformation and/or a reservoir offset from the vertical axis of the conduit. Since in our analyses (this paper) only a vertical degree of freedom is assumed for the location of the pressure source, records related to HERM station together with 1999–2003 records for SPRI and WTYD and 2007–2009 record for WTYD are omitted. For the remaining 29 cGPS velocity measurements the angle between the horizontal velocity and the radial position vector are less than 25· which is considered acceptable.

[12] Combining the radial and vertical components of the station velocities, the apparent depths of pressure sources for each of the 29 combinations are calculated ($D' = (u/w)R$). We employed a bootstrapping algorithm to account for the standard deviations of the measurements [*Chernick*, 1999]. The average (μ) and standard deviation (σ) of the observed vertical and radial surface velocity components, as recorded by cGPS for each epoch, were used to generate ten thousand random samples in the range $\mu \pm \sigma$. These bootstrap datasets were then used to compute the average and standard deviation of the resulting apparent source depth (Figure 2b).

[13] It is noticeable that apparent depth of the reservoir increases from the near-field to the far-field. This is in contrast with the apparent depth-radial distance curves of the pressure sources in the 1D heterogeneous medium (Figure 1b) where the apparent depth decreases slightly with increasing radial distance. In the case of the stiff core model, the apparent depth decreases considerably with increasing distance, which is clearly at odds with the apparent depth measurements inferred from the GPS data themselves. This difference may be explained if at least two pressure sources are geometrically arrayed in a way such that a shallow, weak

pressure source affects the near field, while a strong, deep source influences the far-field observations.

4. Plumbing System Model

[14] We use a model of two vertically stacked chambers implied by a broad suite of observations at SHV. Early cGPS data suggest a shallow chamber at about 5 km [*Aspinall et al.*, 1998; *Barclay et al.*, 1998; *Elsworth et al.*, 2008; *Mattioli et al.*, 1998; *Voight et al.*, 1999] supported by stable crystal phases in erupted magmas to ~130 MPa. Entrained basalt implied a deep source of mafic magma >10 km [*Annen et al.*, 2006; *Murphy et al.*, 1998]. The substantial cumulative volume of the eruption (~1 km^3) and its decade-long continuity and chemical consistency, coupled with observations of co-eruptive displacements, suggest that the upper magma source is voluminous ~4 km^3 [*Voight et al.*, 2006].

[15] To further investigate this model, we inverted the apparent depth data, using two spherical volumetric sources in a heterogeneous half-space. Assuming a Poisson ratio of 0.25 for long term drained deformation, the radial ($\dot{u}$) and vertical ($\dot{w}$) surface velocities will be [*Mogi*, 1958],

$$\dot{u}_{i,j} = \frac{3}{4\pi} \frac{R_i}{\left(R_i^2 + D_j^2\right)^{1.5}} \Delta\dot{V}_j = a_{i,j}\Delta\dot{V}_j \tag{4}$$

$$\dot{w}_{i,j} = \frac{3}{4\pi} \frac{D_j}{\left(R_i^2 + D_j^2\right)^{1.5}} \Delta\dot{V}_j = b_{i,j}\Delta\dot{V}_j \tag{5}$$

Where R and D are the radial and vertical distances of the observation station to pressure sources, $\Delta\dot{V}$ is the volume change rate of the Mogi pressure source, $i = 1\ldots29$ refers to the individual GPS sites and $j = 1, 2$ refers to the shallow and deep pressure sources, respectively. The apparent depth (d) of the Mogi source observed at station i will be

$$d_i = \frac{\dot{w}_{i,1} + \dot{w}_{i,2}}{\dot{u}_{i,1} + \dot{u}_{i,2}} R_i = \frac{b_{i,1}\Delta\dot{V}_1 + b_{i,2}\Delta\dot{V}_2}{a_{i,1}\Delta\dot{V}_1 + a_{i,2}\Delta\dot{V}_2} R_i \tag{6}$$

To take into account the effect of different standard deviations for different stations (Figure 2b) the function being minimized is defined as

$$Er = \sum_{i=1}^{29} \frac{|d_i - D_i|}{\sigma_i^2} \tag{7}$$

where D_i is the observed apparent depth from GPS measurements ($D_i = \frac{w_i^{GPS}}{u_i^{GPS}} R_i$) and σ_i is the standard deviation of the calculated D_i, evaluated using bootstrapping. Since the difference between the calculated apparent depth for the 1D and stiff core models is not significant at distances where most of the measurement stations are located ($R > 3$ km), the transformation function from the 1D models (equation (2)) is used to modify the inversion results to yield a deeper pressure source expected for the heterogeneous system at SHV. A conjugate gradient algorithm is used to minimize the error function (equation (7)) [*Press et al.*, 1992]. The variables involved are the depths (D_j) and volume changes (ΔV_j) of the two pressure sources. The objective function is minimized to yield a best-fit source geometry of a shallow magma reservoir at 5 km depth with 0.012 km^3 volume change, together with a deep magma reservoir at 17 km depth with 0.25 km^3 volume change. These calculated volume changes result from the minimization of all combined eruption and repose data serve only to identify that (i) the inflationary-deflationary episodes of the deep reservoir are synchronous with repose and eruptive periods, respectively, (ii) the volume changes in the shallow reservoir are more than an order-of-magnitude smaller than those of the deep reservoir, and that (iii) these deformations of the shallow reservoir are only apparent close to the volcano and are completely masked by deformations of the deep chamber at radii greater than approximately the depth of the deep chamber. The apparent depth vs. radial distance curve resulting from the inversion is plotted in Figure 2b suggesting that the proposed dual chamber structure can explain the apparent depth contrast between near-field and far-field observation points provided that the deep chamber undergoes volume changes an order of magnitude larger than the shallow chamber. Single reservoir geometries, such as oblate or prolate spheroids cannot explain the few kilometers difference in the observed apparent depths predicted by the proximal and distal stations. Alternative reservoir geometries, such as vertically-oriented cigar-like chambers are better able to represent near-crater subsidence (Voight et al., submitted manuscript, 2010) but provide no better fits either in the far-field or in representing deformation between successive inflationary or deflationary epochs.

5. Discussion and Conclusion

[16] We used results from a seismic imaging experiment and the resulting velocity tomography to constrain axisymmetric elastically heterogeneous models for Soufriere Hills Volcano. Based on the results from the seismic tomography, two sets of models were explored. In the first set, a continuously varying stiffness profile was assumed based on an averaged velocity profile, while the second set included a stiff core underneath the crater. Both end-members models were conditioned based on the SEA-CALIPSO inversion results (Shalev et al., submitted manuscript, 2010). Introducing the "apparent depth' of the pressure source, we show that the inversions of geodetic data in these models yield deeper pressure sources than models which only consider a homogeneous half-space. In addition, given that the inferred source for any given surface velocity field will be deeper for heterogeneous versus homogeneous crustal models, the required reservoir overpressure (or change in reservoir volume) will also be higher. Thus the assumption of a homogeneous elastic crust underestimates both the depth and excess pressure of the deformation source. For the case of SHV, a linear function was found to transform the inversion results of a spherical pressure source depth within the homogenous medium to the more realistic inhomogeneous case.

[17] During the eruption episode of 1995–1998 and the subsequent pause episode of 1998–1999, none of the available GPS sites could yield an apparent depth of the pressure source with an appropriate tolerance ($\sigma < 3500$ m) using our procedure. Our analysis therefore shows that the quality of cGPS data has improved significantly at SHV since 1995, and in particular using the exceptionally robust and stable CALIPSO installations post-2003.

[18] The SHV geodetic data suggest that the apparent depth of the source increases with increasing radial distance from the volcano. This observation is consistent with a dual reservoir plumbing system, with the deeper reservoir undergoing volume changes an order of magnitude larger than the shallow reservoir. Our best-fit model combines a shallow reservoir centered at 5 km and a deep reservoir at 17 km, the latter changing volume about 20 times faster than the former. Our results are qualitatively similar to prior inversion results for SHV [*Elsworth et al.*, 2008] in which dual-reservoir plumbing systems is inferred and the deep reservoir is shown to be inflating or deflating an order of magnitude faster than the shallow one. Given the high level of uncertainty involved in the evaluation of the apparent depths (Figure 2b), it is not possible to assess the geometry of the SHV plumbing system nor the inferred volume changes in great detail.

[19] **Acknowledgments.** This work is a partial result of support by the National Science Foundation under awards NSF-CMS-9908590, NSF-CD-0607691, NSF-CD-0507334, and NSF-CD-0607782. The Caribbean Andesitic Lava Island Precision Seismo-geodetic Observatory (CALIPSO) facility was supported by grants NSF-IF-0523097 and NSF-IF-0732728, and this support is gratefully acknowledged. The manuscript benefited from reviews by Mike Poland and one anonymous reviewer. The conclusions reported here are those of the authors.

References

Amoruso, A., L. Crescentini, A. T. Linde, I. S. Sacks, R. Scarpa, and P. Romano (2007), A horizontal crack in a layered structure satisfies deformation for the 2004–2006 uplift of Campi Flegrei, *Geophys. Res. Lett.*, *34*, L22313, doi:10.1029/2007GL031644.

Amoruso, A., L. Crescentini, and G. Berrino (2008), Simultaneous inversion of deformation and gravity changes in a horizontally layered halfspace: Evidences for magma intrusion during the 1982–1984 unrest at Campi Flegrei caldera (Italy), *Earth Planet. Sci. Lett.*, *272*(1–2), 181–188, doi:10.1016/j.epsl.2008.04.040.

Annen, C., J. D. Blundy, and R. S. J. Sparks (2006), The genesis of intermediate and silicic magmas in deep crustal hot zones, *J. Petrol.*, *47*(3), 505–539, doi:10.1093/petrology/egi084.

Aspinall, W. P., A. D. Miller, L. L. Lynch, J. L. Latchman, R. C. Stewart, R. A. White, and J. A. Power (1998), Soufrière Hills eruption, Montserrat, 1995–1997: Volcanic earthquake locations and fault plane solutions, *Geophys. Res. Lett.*, *25*(18), 3397–3400, doi:10.1029/98GL00858.

Barclay, J., M. J. Rutherford, M. R. Carroll, M. D. Murphy, J. D. Devine, J. Gardner, and R. S. J. Sparks (1998), Experimental phase equilibria constraints on pre-eruptive storage conditions of the Soufrière Hills magma, *Geophys. Res. Lett.*, *25*(18), 3437–3440, doi:10.1029/98GL00856.

Bianchi, R., A. Coradini, C. Federico, G. Giberti, P. Lancian, J. P. Pozzi, G. Sartoris, and R. Scandon (1987), Modeling of surface deformation in volcanic areas: The 1970–1972 and 1982–1984 crises of Campi Flegrei, Italy, *J. Geophys. Res.*, *92*(14), 139–150.

Bonaccorso, A., S. Cianetti, C. Giunchi, E. Trasatti, M. Bonafede, and E. Boschi (2005), Analytical and 3-D numerical modelling of Mt. Etna (Italy) volcano inflation, *Geophys. J. Int.*, *163*(2), 852–862, doi:10.1111/j.1365-246X.2005.02777.x.

Brocher, T. A. (2005), Empirical relations between elastic wavespeeds and density in the earth's crust, *Bull. Seismol. Soc. Am.*, *95*(6), 2081–2092, doi:10.1785/0120050077.

Chernick, M. R. (1999), *Bootstrap Methods: A Practitioner's Guide*, John Wiley, New York.

Crescentini, L., and A. Amoruso (2007), Effects of crustal layering on the inversion of deformation and gravity data in volcanic areas: An application to the Campi Flegrei caldera, Italy, *Geophys. Res. Lett.*, *34*, L09303, doi:10.1029/2007GL029919.

Elsworth, D., G. Mattioli, J. Taron, B. Voight, and R. Herd (2008), Implications of magma transfer between multiple reservoirs on eruption cycling, *Science*, *322*(5899), 246–248, doi:10.1126/science.1161297.

Mattioli, G. S., and R. Herd (2003), Correlation of cyclic surface deformation recorded by GPS geodesy with surface magma flux at Soufrière Hills volcano, Montserrat, *Seismol. Res. Lett.*, *74*(2), 230.

Mattioli, G. S., T. H. Dixon, F. Farina, E. S. Howell, P. E. Jansma, and A. L. Smith (1998), GPS measurement of surface deformation around Soufrière Hills volcano, Montserrat from October 1995 to July 1996, *Geophys. Res. Lett.*, *25*(18), 3417–3420, doi:10.1029/98GL00931.

Mattioli, G. S., et al. (2004), CALIPSO project at Soufrière Hills Volcano, Montserrat: Prototype PBO instrumentation installed and captures massive dome collapse of July 2003, *Eos Trans. AGU*, *85*(34), doi:10.1029/2004EO340001.

Mattioli, G. S., R. A. Herd, M. H. Strutt, G. Ryan, C. Widiwijayanti, and B. Voight (2010), Long term surface deformation of Soufrière Hills Volcano, Montserrat from GPS geodesy: Inferences from simple elastic inverse models, *Geophys. Res. Lett.*, doi:10.1029/2009GL042268, in press.

Mogi, K. (1958), Relations between the eruptions of various volcanoes and the deformations of the ground surfaces around them, *Bull. Earthquake Res. Inst. Univ. Tokyo*, *36*, 99–134.

Murphy, M. D., R. S. J. Sparks, J. Barclay, M. R. Carroll, A. M. Lejeune, T. S. Brewer, R. Macdonald, S. Black, and S. Young (1998), The role of magma mixing in triggering the current eruption at the Soufrière Hills volcano, Montserrat, West Indies, *Geophys. Res. Lett.*, *25*(18), 3433–3436, doi:10.1029/98GL00713.

Nafe, J. E., and C. L. Drake (1957), Variation with depth in shallow and deep water marine sediments of porosity, density and the velocities of compressional and shear waves, *Geophysics*, *22*, 523–552, doi:10.1190/1.1438386.

Newman, A. V., T. H. Dixon, G. I. Ofoegbu, and J. E. Dixon (2001), Geodetic and seismic constraints on recent activity at Long Valley Caldera, California: Evidence for viscoelastic rheology, *J. Volcanol. Geotherm. Res.*, *105*(3), 183–206, doi:10.1016/S0377-0273(00)00255-9.

Press, W. H., et al. (1992), *Numerical Recipes in C*, 2nd ed., Cambridge Univ. Press, Cambridge, U. K.

Trasatti, E., C. Giunchi, and M. Bonafede (2005), Structural and rheological constraints on source depth and overpressure estimates at the Campi Flegrei caldera, Italy, *J. Volcanol. Geotherm. Res.*, *144*(1–4), 105–118, doi:10.1016/j.jvolgeores.2004.11.019.

Voight, B., et al. (1999), Magma flow instability and cyclic activity at Soufrière Hills Volcano, Monsterrat, British West Indies, *Science*, *283*(5405), 1138–1142, doi:10.1126/science.283.5405.1138.

Voight, B., et al. (2006), Unprecedented pressure increase in deep magma reservoir triggered by lava-dome collapse, *Geophys. Res. Lett.*, *33*, L03312, doi:10.1029/2005GL024870.

Wadge, G., R. Herd, G. Ryan, E. S. Calder, and J.-C. Komorowski (2010), Lava production at Soufrière Hills Volcano, Montserrat: 1995–2009, *Geophys. Res. Lett.*, *37*, L00E03, doi:10.1029/2009GL041466.

Widiwijayanti, C., A. Clarke, D. Elsworth, and B. Voight (2005), Geodetic constraints on the shallow magma system at Soufriere Hills Volcano, Montserrat, *Geophys. Res. Lett.*, *32*, L11309, doi:10.1029/2005GL022846.

D. Elsworth and R. Foroozan, Department of Energy and Environmental Engineering, G3 Center and EMS Energy Institute, Pennsylvania State University, 110 Hosler Bldg., University Park, PA 16802, USA. (rzforoozan@gmail.com)

G. S. Mattioli, Department of Geosciences, University of Arkansas, 113 Ozark Hall, Fayetteville, AR 72701, USA.

B. Voight, Department of Geosciences, Pennsylvania State University, Deike Bldg., University Park, PA 16802, USA.